ELSEVIER

Journal of Nuclear Materials 278 (2000) 64–72

journal of nuclear materials

www.elsevier.nl/locate/jnucmat

The effect of amorphization on the Cs ion exchange and retention capacity of zeolite-NaY

B.X. Gu, L.M. Wang, R.C. Ewing *

Department of Nuclear Engineering and Radiological Sciences, University of Michigan, Ann Arbor, MI 48109-2104, USA

Received 15 June 1999; accepted 11 August 1999

Abstract

Zeolite-NaY is susceptible to both irradiation- and thermally-induced amorphization. Amorphized zeolite-NaY loses approximately 95% of its ion exchange capacity for cesium due to the loss of exchangeable cation sites and /or the blockage of access to exchangeable cation sites. A secondary phase was formed during the ion exchange reaction with cesium. The Cs-exchanged zeolite-NaY phase has a slightly higher thermal stability than the unexchanged zeolite-NaY. A desorption study indicated that the amorphization of cesium-loaded zeolite-NaY enhances the retention capacity of exchangeable Cs ions due to the closure of structural channels.

1. Introduction

Reversible cation exchange is one of the most important properties of zeolites. This is the basis for using zeolites in the selective removal of radionuclides, such as cesium, strontium, rare-earths and actinides from the high-level liquid nuclear waste [1]. A variety of waste treatment systems, employing zeolite ion exchangers, have been developed for processing high-level liquid waste generated from nuclear fuel reprocessing [2,3], low level liquid waste from nuclear power plants [4], as well as the liquid waste from decontamination and decommissioning of nuclear facilities. Examples include decontamination of various radioactive liquid wastes generated during decommissioning activities at the former nuclear fuel reprocessing plant at West Valley, New York [5] and decontamination of highly radioactive water resulting from the accident at Unit 2 of the Three Mile Island nuclear power station [6]. Zeolites loaded with radionuclides can either be incorporated into borosilicate glass to form a waste form or thermally treated without addition of a solidifying agent to form a glass or new phases that may be suitable for long term disposal in a geological repository [7]. For instance, Cs- and Sr-exchanged zeolites can be recrystallized to stable aluminum silicates by thermal treatment at temperatures above 900°C. Hydrothermal treatment of zeolites loaded with Cs and Sr at lower temperatures (200–400°C) can form pollucite [8,9]. Zeolite is also a potential back-fill material in nuclear waste repositories [10]. Zeolites are present in volcanic tuffs at the Yucca Mountain nuclear waste repository, and they may play an important role in retarding radionuclide transport [11]. As zeolites are intended to retain radionuclides, they will receive considerable radiation doses over time, and the cumulative doses in zeolites utilized as exchange media, waste forms, or near-field back-fill can be substantial. At Three-Mile Island, on-site sampling of zeolite columns indicated that gases (oxygen and hydrogen) were generated as a result of radiolysis [6]. For commercial high-level nuclear waste forms with a 25 wt% waste loading, the cumulative ionization dose from beta decay can be as high as 10^{10} Gy after 100 years, and the anticipated dose from α-decay may reach 7×10^8 Gy in only 1000 years [12]. A number of studies [13–22] have reported that zeolites are susceptible to various types of radiation damage. At room temperature, analcime, natrolite and zeolite-Y, become completely amorphized at an ionizing dose in the range of 3.2×10^{10}–1.6×10^{11} Gy, and the dose required for amorphization decreases with increasing temperature due to the thermal instability of the zeolites [19]. Analcime and zeolite-5A were found to

* Tel.: +1-734 647 8529; fax: +1-734 647 8531.
E-mail address: rodewing@umich.edu (R.C. Ewing).

0022-3115/00/$ - see front matter
PII: S0022-3115(99)00224-X

lose their long-range order at doses of 0.1 dpa and $\sim 6 \times 10^8$ Gy with 1–1.5 MeV krypton irradiation [20,21]. Structural damage in zeolite-A has been detected under neutron irradiation. Complete collapse of the crystalline structure occurred when the dose reached 7×10^{23} n/m^2 [22]. Based on these results, zeolites in the near-field of a waste repository may be amorphized within 1000 years after waste emplacement, and this time period is short as compared to a 10 000 year compliance period for a nuclear waste repository. Therefore, changes in zeolite properties, such as the ion exchange and elemental retention capacities, as a result of the radiation-induced crystalline-to-amorphous transition are significant in evaluating the long-term performance of zeolite phases.

Temperature also affects the structure and properties of zeolites. Most zeolites become dehydrated upon heating and many undergo the crystalline-to-amorphous transition at temperatures of 400–900°C, depending on the type of zeolite. A gradual breakdown of the zeolite framework has been observed when zeolite-Y was heated in air from 300°C to 1100°C [23]. Dehydroxylation and light cation evaporation may be responsible for the disruption of the zeolite-Y structure [24]. In the case of nuclear waste, significant heating is possible after waste emplacement in a repository. Heat generated from decay of the fission products can result in an initial storage temperature as high as 600°C, and the temperature may still be as high as 300°C after 100 years of storage [12]. As indicated by Wang et al. [19], high temperatures combined with high radiation doses result in the acceleration of damage to zeolite structures.

The cation exchange behavior of zeolite depends on the nature of the cation species, size, and charge, as well as the structure of the zeolite. Radiation- or thermally-induced amorphization dramatically changes the structure, which, in turn, leads to cation site redistribution and a change of the framework charge. The collapse of the framework structure may also reduce the number of accessible cation sites by blocking the open channels and reducing the effective surface area. Consequently, the ion exchange and retention behavior of zeolites may be affected significantly by the amorphization process. Extensive experimental studies of ion exchange of radionuclides in zeolites have been performed over the last few decades [25–27]. However, these studies have been focused only on the effects of time, temperature, solution chemistry and pH. The effects of radiation- or thermally-induced amorphization on ion exchange capacity have not been considered in these studies. There have been only a few studies conducted to investigate the effects of irradiation on the ion exchange capacity of zeolites. A study of the exchange capacity of cesium by a synthetic zeolite, Ionsiv IE-95, showed no significant change after a cumulative gamma-dose of 1.1×10^8 Gy [28]. Gamma irradiation of zeolite-4A also showed no effect on structure and Co-sorption behavior at a cumulative dose of 1×10^6 Gy [29]. Irradiation of the same material by either a gamma source or a neutron source, however, caused a slightly reduced cesium uptake which was attributed to the displacement of exchangeable cations to 'locked-in' sites [30,31]. Although the same cation-displacement mechanism was suggested for zeolite-13X, no alteration of the ion exchange capacity was detected [32]. The contradictions among these results may be related to insufficient damage having been produced by the radiation and that the measurement of sorption capacity change may not be sensitive to minor structural changes. Because of the practical difficulties involved in completing experiments at high dose rates and accumulating total doses up to 10^{10}–10^{11} Gy with bulk material, there have been no studies of the effect of long term radiation-induced amorphization on zeolite ion exchange and elemental retention behavior.

In the present study, crystalline zeolite-NaY and Cs-exchanged zeolite-NaY were transformed to the amorphous state by thermal treatment at temperatures of 900–1000°C. Although the amorphous phase produced by thermal treatment may not have exactly the same properties as those obtained by irradiation, the processes of thermally- and radiation-induced amorphization have many common features. For example, both processes can cause cation migration, the loss of structural water, and the collapse of the framework structure. Therefore, a comparison of adsorption and desorption behavior of crystalline and amorphous zeolites is useful for the evaluation of the effect of irradiation on zeolite properties.

2. Experimental

2.1. Materials

Zeolite-NaY (Si/Al = 2.55) that contained 13.0 wt% Na_2O was supplied by Zeolyst International Company in the form of powder with the sizes less than one micron. The surface area of the zeolite powder was 900 m^2/g. The chemical composition of the zeolite-NaY is: $NaAlSi_2O_6{\cdot}nH_2O$. Zeolite-Y and faujasite have a topologically similar aluminosilicate framework structure, and both are assigned to the faujasite-type structure. As illustrated in Fig. 1(A), there are three different types of cages in the faujasite-type structure: supercages, sodalite cages (or β cage), and double 6-ring prisms. A supercage is connected to four other supercages via a 12-ring window with a free aperture of 0.77 nm. The sodalite cages, which are connected to four adjoining supercages via 6-ring openings of 0.22 nm, are linked together by the double 6-ring prisms. Exchangeable cations are located in all three types of cages. Fig. 1(B) shows the possible positions that can be occupied by the cations.

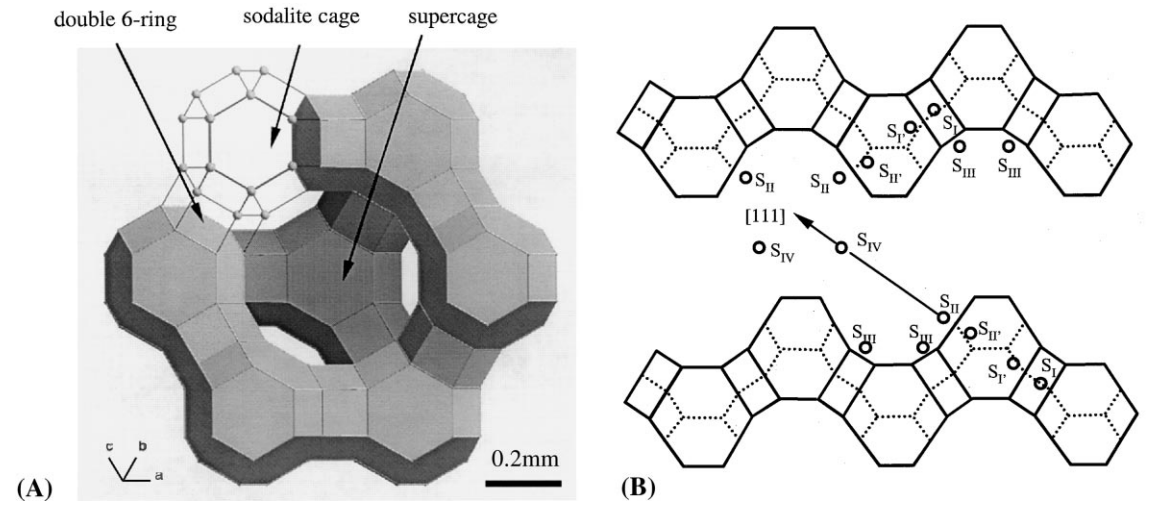

Fig. 1. Schematic diagram of faujasite-type structure and cation distribution. (A) The structure viewed along the [1$\bar{1}$1] direction. (B) Cation sites in faujasite-type structure: site I is located in the center of double 6-ring. Site I′ and II′ are located inside the sodalite cages. Sites II, III, and IV refer to different locations inside the supercages [22].

The distribution of cations depends not only on the properties of each cation, but also on the level of dehydration. The size of the free aperture plays an important role in determining the features of the ion exchange reaction for particular cations. Approximately two-thirds of the exchangeable cation sites are located in supercages. Earlier results have shown that only 68% of the Na in the structure can be exchanged with Cs because Cs ions can only enter the supercages, and the apertures of the sodalite cages and the double 6-ring prisms are too small for the Cs ions to enter [22].

Cesium-loaded zeolite was prepared by ion exchange. For the ion exchange, all the Cs^+ solutions were prepared by dissolving reagent grade CsCl into distilled and deionized water. One gram of zeolite was placed in contact with 0.5M of CsCl aqueous solution for 24 h at room temperature. The mixture was filtered using 0.45 μm filter paper and dried in air at 50°C for 48 h. Cesium content in the Cs-exchanged zeolite was analyzed using neutron activation analysis, for which the sample was first irradiated in the Ford Nuclear Reactor (FNR) at University of Michigan, and then analyzed using a gamma counter. The concentration of Cs was 21 wt.% before heat treatment. Both zeolite-NaY and the cesium-exchanged zeolite-NaY were heated in air at elevated temperature (800–1000°C) to form amorphous structure.

2.2. Experimental procedures

2.2.1. Powder X-ray diffraction (XRD) and electron microscopy

The atomic structures of zeolite-NaY and Cs-exchanged zeolite-NaY, before and after thermal treatment, were examined by means of powder X-ray diffraction. The XRD spectra were obtained using Cu-Kα radiation ($\lambda = 0.15405$ nm). The structures of zeolite-NaY and Cs-loaded zeolite were investigated with a JEM 2000FX transmission electron microscope (TEM). Zeolite powders were crushed and suspended on a holey-carbon film supported by copper grids. The electron energy was 200 keV, and all the samples were irradiated at a dose rate of 2.5×10^{21} e^-/m^2 s at room temperature. The effect of thermal treatment on the morphologies of zeolite-NaY and zeolite-NaCsY was examined using a scanning electron microscope, Philips FEG SEM. The zeolite powders were mounted on the sample holder by conductive carbon glue and coated with a carbon film. The microscope was operated at a voltage of 10 keV.

2.2.2. Ion exchange

For both kinetic and equilibrium studies, the ion-exchange experiments used 10 mg of crystalline zeolite or 100 mg of amorphized zeolite powder in contact with 25 ml CsCl solution. The mixtures were continuously stirred on a Lab-Line shaker with an orbital speed of 150 rpm. All the ion exchange experiments were performed at room temperature. The pH values of the solution were measured before and after the exchange.

In the kinetic studies, the ion exchange capacities of zeolite-NaY, with and without thermal treatment, were measured as a function of time in a 1mM CsCl solution. After various preset time intervals, centrifugation at 10 000 rpm was applied to separate the liquid phase from the solid. Samples of supernatant were analyzed for Cs^+ content by atomic absorption spectrophotometry. The reaction time obtained from the kinetic studies was used

in the subsequent equilibrium studies to determine the time necessary to ensure equilibrium.

In the equilibrium studies, the ion-exchange isotherms for Cs-zeolite reaction were obtained in the CsCl solution with concentrations of 0.2 to 2mM. The equilibrations were performed at room temperature under thoroughly stirred conditions. The zeolite-solution mixture was centrifuged at equilibrium, and the aliquot of the supernatant solution was analyzed by atomic absorption.

2.2.3. Desorption

A 10 mg zeolite sample loaded with cesium was put in contact with 25 ml of deionized water for 1, 2, 4, 7, 14 and 25 days, respectively. The mixtures were continuously stirred on a lab-line orbital shaker with the speed controlled at 150 rpm. Sample temperature was maintained at room temperature over the entire desorption period. The cesium content in the liquid phase was analyzed by atomic absorption to determine the amount of Cs released. The same experiment was also conducted with cesium-exchanged samples that were heated at 900°C and 1000°C in air for 30 min to form partially and fully amorphized phases, respectively.

3. Results and discussion

3.1. Structure change due to thermal treatment and electron beam irradiation

The atomic structures of the zeolite-NaY and ion-exchanged zeolites were investigated using XRD and TEM. The powder diffraction data obtained for zeolite-NaY are in agreement with the results of Breck [22]. The XRD patterns in Fig. 2 show the transition from crystalline-to-amorphous state due to thermal treatment. When heated at 800°C for 40 min followed by cooling in air, the zeolite showed a reduced peak intensity in the XRD spectrum; however, the position and relative intensity of individual peaks remained constant. Zeolite-NaY was completely amorphized at 900°C. A further increase in temperature to 1000°C resulted in melting and the formation of a glass. The XRD pattern for zeolite-NaY treated at 1000°C has the same profile as that obtained at 900°C. The zeolite sample that was thermally treated at 900°C was used in the subsequent ion exchange experiment.

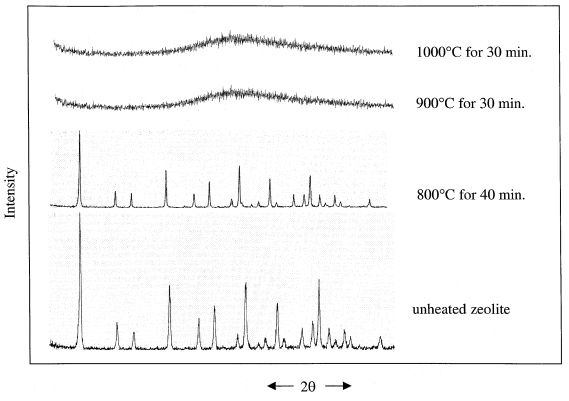

Fig. 2. X-ray diffraction patterns for zeolite-NaY, unheated and heated at 800°C, 900°C, 1000°C.

The crystalline-to-amorphous transformation has also been observed for zeolite-NaY during the TEM experiment. Fig. 3 is a sequence of TEM diffraction patterns of zeolite-NaY taken at different cumulative electron doses. The 200 keV electron beam interacted with the zeolite sample at a dose rate of approximately 2.5×10^{21} e^-/m^2 s. A gradual loss of diffraction spots in the diffraction patterns indicated that the crystalline structure was destroyed progressively with the increase in radiation dose. Csencsits and Gronsky [13], have performed a computer simulation of the TEM image of an amorphous cell for zeolite-Y. The results showed that there was no periodicity in the structure, i.e. the structure was completely random. Full amorphization was achieved at a dose of 4.0×10^{23} e^-/m^2 at room temperature. The error involved in the measurement of amorphization dose was ±30% and may be attributed to inhomogeneous particle size or sample thickness. Yokota et al. [17] have reported that the complete amorphization dose for the natural zeolite mesolite is proportional to crystal size. The amorphous region starts to form from the edge of crystal and advances perpendicular to the specimen surface with time. Thus, the required amorphization dose increases with the increase of sample thickness [17].

The processes of thermal- and irradiation-induced amorphization are similar in several aspects. First, both the thermal treatment and irradiation cause the collapse of the framework structure. Zeolite-NaY was found to lose its crystalline structure over a narrow temperature interval of 760–800°C after prolonged heating for 16 h [22]. The collapse of the framework structure is evident by the dramatic decrease of surface area (on the order of one to two orders of magnitude) [7] and the decrease in volume [16]. The destruction of the crystal structure is also accompanied by a change in particle morphology. Fig. 4 shows the SEM images of zeolites before and after thermal treatment. The morphological change in the amorphized zeolites was significant. The bead-like shape of the amorphized zeolites (Fig. 4(B)) is different from the original cubic form (Fig. 4(A)). Similar phenomena have been observed in zeolite-L after irradiation to a dose of 10^{25} e^-/m^2 [16]. The mechanisms involved in the thermally induced amorphization usually include the weakening of chemical bonds in the framework structure, decomposition and dehydroxylation. Several

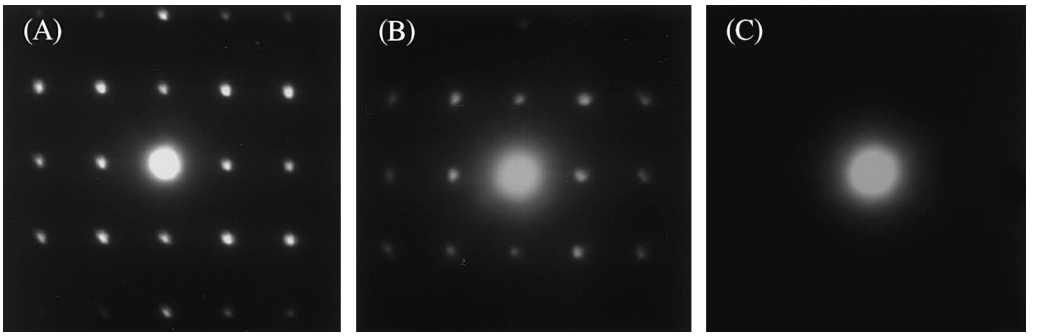

Fig. 3. Sequence of selected-area diffraction patterns of zeolite-NaY during 200 KeV electron beam irradiation: (A) unirradiated; (B) 3.0×10^{23} e^-/m^2; (C) 4.0×10^{23} e^-/m^2.

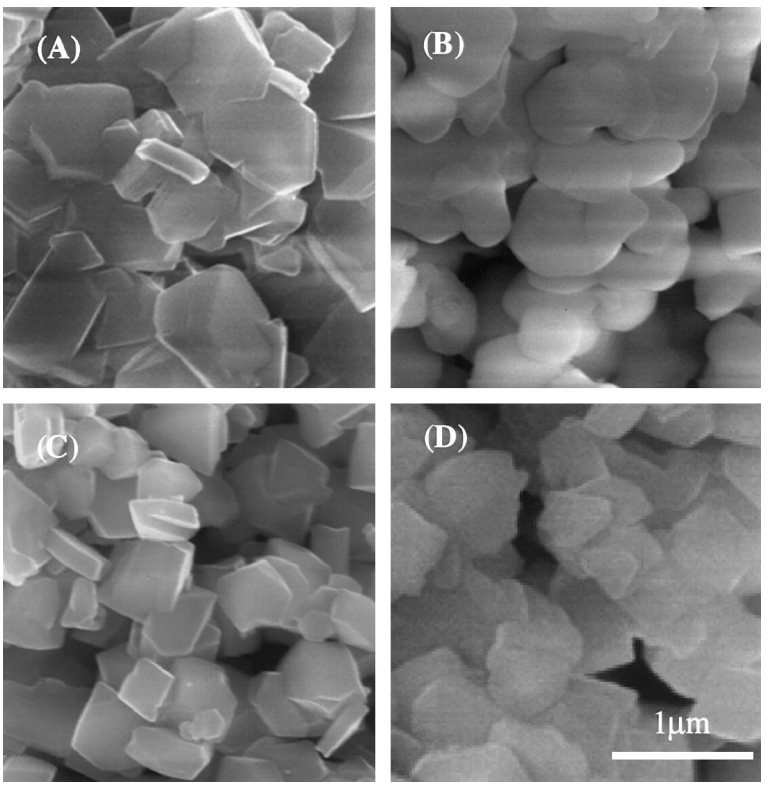

Fig. 4. SEM images of zeolite-NaY and zeolite-NaCsY before and after thermal treatment. (A) zeolite-NaY unheated; (B) zeolite-NaY heated at 900°C; (C) Zeolite-NaCsY unheated; (D) zeolite-NaCsY heated at 900°C.

studies have confirmed that the damage of zeolites by the electron beam is dominated by a radiolytic decomposition mechanism [13,16,21]. Radiolytic damage involves the transfer of energy from the incident electron to the electrons in the specimen, which may cause bonds to break. Treacy [16] has proposed that ionization of structural water in zeolite could produce radicals that weaken bonds in the aluminosilicate framework, and this initiates collapse of the framework. As speculated by Acosta et al. [33], the amorphization of zeolite-CaA under electron beam irradiation starts from very localized sites, such as the apertures of the channels, i.e. the apertures of the channels are more susceptible to radiation damage. This speculation is supported by the changes in the dimensions of the channels observed from high resolution TEM images and is further supported by the fact that the edges of the crystallites are more easily damaged at the early stage of radiation damage.

Secondly, dehydration has been observed in the course of both radiation- and thermally-induced amorphization. Water loss is a major cause of the compositional modification in the electron beam-damaged zeolite [16]. The displacement of water molecules from the zeolite structure has been confirmed by HRTEM investigations [18,21]. The water molecules can be displaced either by direct collision or ionization. A loss of structural water has also been found in the neutron-irradiated zeolite [31]. An earlier study [22] showed that zeolite-Y undergoes dehydration reversibly and continuously at temperatures lower than 300°C with no significant change in the topology of the framework structure. A substantial loss of molecular water occurred only over the temperature range for which the zeolite was completely dehydrated. Finally, cation migration occurs during irradiation and thermal treatment. The positions of the cations are often temperature-dependent. When structural water is driven from the structure by heating, cations may move from one type of cation site to another. Sodium was found to migrate from sodalite cages into supercages upon dehydration at >350°C in the cesium-exchanged zeolite-Y [34]. Radiation-induced cation migration has been observed in zeolite-L under electron irradiation [16]. Cation concentrations in the radiation damaged area have been found to be 10–60% lower, as determined by energy-dispersive X-ray spectroscopy, than the overall concentration as measured by chemical methods, indicating that the cations have migrated away from the probed region under the influence of the electron beam.

The XRD spectra of cesium-exchanged zeolite before and after thermal treatment are shown in Fig. 5. The loaded Cs concentration is 21 wt%. The exchange of Cs for Na in the zeolite structure results in reduced peak intensity, as compared with zeolite-NaY. This change is primarily due to the change in X-ray diffraction structure factors caused by introducing Cs into the crystalline structure. In addition to the peaks corresponding to the original zeolite-NaY, extra peaks were found to be present in the XRD spectrum, indicating that a secondary phase may have formed when zeolite-NaY was exchanged with Cs. The secondary phase is probably a cesium-rich aluminum silicate, yet, none of the known cesium silicate phases in International Center for Diffraction Data (ICDD) database matches the peak file. After heating at 900°C for 30 min, the diffraction maxima that correspond to zeolite-NaY at lower values of 2θ disappeared. Increasing the temperature to 1000°C resulted in the disappearance of all remaining peaks and a fully amorphized structure. This result indicates the existence of a secondary crystalline phase that has a higher thermal stability than the original structure. The different thermal stabilities between the Cs-exchanged phase and the original zeolite phase can also be seen in the SEM images in Fig. 4. When heated to 900°C, the shape of zeolite-NaY particles became spherical, while the majority of Cs-exchanged zeolite particles remain unchanged. Significant morphological change occurred when zeolite-NaCsY was thermally treated at 1000°C. The formation of two solid phases has been observed in ion exchange reaction of zeolite-X with strontium [22]. A strontium-rich expanded zeolite phase was identified by optical microscopy. The nature of the exchanged cations was also found to be important in determining the stability and dehydration behavior of zeolites [22]. As the size of univalent cation increases, the temperature at which the water is lost increases. This phenomenon may be due to the filling of void space in the zeolite structure by the cations after the removal of water.

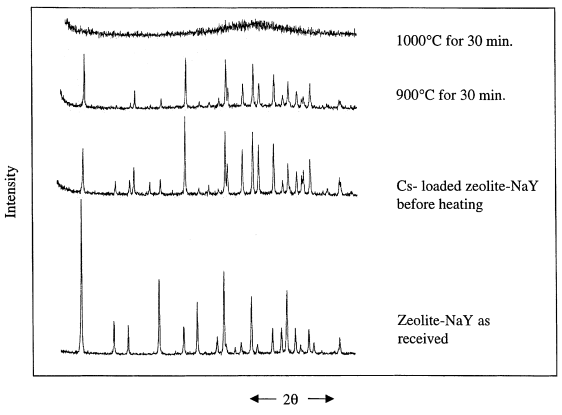

Fig. 5. X-ray diffraction patterns for zeolite-NaCsY, unheated and heated at 900°C, 1000°C. The XRD pattern of the original zeolite-NaY is shown for comparison.

Cs-loaded zeolite was also found to undergo the crystalline-to-amorphous transition when it was exposed to an electron beam at a similar dose rate as used in the zeolite-NaY case. The critical accumulated dose at which the material became fully amorphous was 5.0×10^{23} e^-/m^2. This value is slightly higher than that obtained for zeolite-NaY, indicating that Cs-exchanged zeolite is more stable under irradiation. However, the difference may also be attributed to the error ($\sim\pm30\%$) involved in the measurements, because the amorphization dose may be affected by the particle size or the thickness of the sample exposed to the electron beam.

3.2. Ion exchange

In kinetic studies, the ion exchange capacity of crystalline and amorphous zeolite–NaY with cesium was measured as a function of time in 1mM CsCl solution. The pH value of the original CsCl solution was 7.5 and no significant change in pH value (within ±0.5) was observed after ion exchange. The Cs–Na exchange reaction on crystalline zeolite reached equilibrium quickly (in less

than 5 min) under continuous stirring conditions, and approximately 50% of the sodium was replaced by cesium. The fast reaction rate and incomplete exchange indicated that the majority of the ion exchange occurred only in supercages where the free aperture is large enough for cesium ions to reach the exchangeable cation sites. Similar results have been reported for zeolite-X and zeolite-A under similar conditions [35]. As shown in Fig. 6, amorphized zeolite-NaY has a much lower exchange capacity for Cs as compared with the undamaged, crystalline zeolite. In fact, the ion exchange capacity drops to almost zero after the zeolite is fully amorphized. This result implies that zeolite has lost almost all the exchangeable cation sites upon the collapse of crystalline structure to amorphous state. In the zeolite structure, the fundamental unit is a tetrahedrally coordinated small cation, such as Si^{4+}. The substitution of aluminum for silicon produces a deficiency in valence charge that must be locally balanced by the presence of an additional positive ion within the interstices of the structure. These interstitial sites form the basis of the exchangeable cation sites. When the framework structure collapses, the chemical bonds between silicon and oxygen, or aluminum and oxygen, are broken and local charge balance is lost. As a result, the exchangeable cation sites no longer exist. Another possible explanation for the low exchange capacity of amorphized zeolite is the closure of the open channels leading to exchangeable cation sites. As speculated by Acosta et al. based on HRTEM [33], the entrances of the channels are more susceptible to radiation damage than other parts of the structure. Damage often occurs at channel entrances at the early stage of irradiation. In this case, exchangeable cations are likely to be trapped inside the cages, and Cs^{+} cannot diffuse into the structure to exchange with them.

The equilibrium study was carried out by placing zeolite samples in contact with CsCl solution with initial concentrations in the range of 0.2 and 2mM. At equilibrium, the cesium concentration of the solution phase was analyzed, and the mass of solute sorbed per unit mass of sorbent (Q_e) was calculated from

$$Q_e = \frac{(C_o - C_e) \times L}{M_z}, \tag{1}$$

where C_o is the original solution concentration, C_e the equilibrium solution concentration, L the volume of the solution in contact with zeolite, and M_z the mass of zeolite used in each experiment.

The ion-exchange isotherms for the crystalline and amorphous zeolites were obtained by plotting Q_e as a function of C_e (Fig. 7). The nonlinear isotherm profile for the crystalline zeolite indicates a favorable exchange of Na in zeolite-NaY by Cs in solution, which is in agreement with previous results [36]. The amorphous zeolite has a linear isotherm with low ion exchange capacities (<0.1 meq/g). The linear isotherm has been found most commonly in the systems for which the sorbents have a low sorption potential [37].

3.3. Desorption

Cesium-exchanged zeolite-NaY, without thermal treatment as well as thermally treated at 900°C and 1000°C, has been studied in a desorption experiment. Fig. 8 shows the change of desorption rate of cesium in deionized water as a function of time. The sample without thermal treatment gives the highest desorption rate among all three of Cs-exchanged zeolite-NaY samples, while the fully amorphized zeolite obtained at

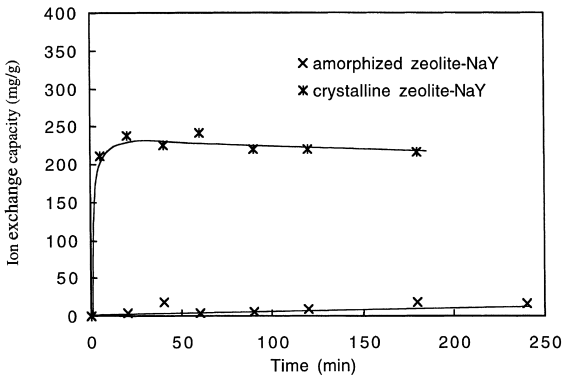

Fig. 6. Comparison of ion exchange capacities of crystalline and amorphous zeolite-NaY. The amorphous phase was obtained by thermal treatment at 900°C. The experiment was conducted in 1 mM CsCl solution at room temperature.

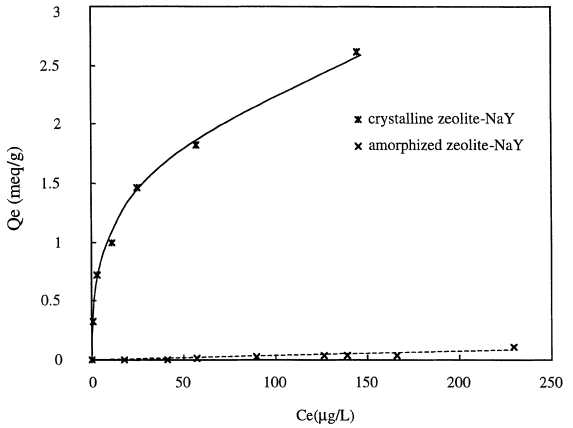

Fig. 7. Ion exchange isotherms for CsCl with crystalline zeolite-NaY and amorphous zeolite-NaY obtained by thermal treatment at 900°C. The experiment was performed at room temperature.

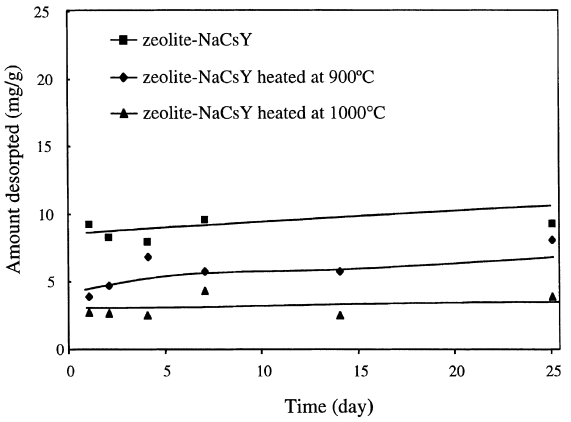

Fig. 8. Desorption of cesium ions from unheated zeolite-NaCsY and zeolite-NaCsY thermally treated at 900°C and 1000°C. The experiment was conducted at room temperature in deionized water.

1000°C exhibits the lowest desorption rate. This phenomenon can be explained by the closure of open channels in the structure during the crystalline-to-amorphous transformation. Apparently, the collapse of channel openings either by thermal treatment or irradiation can block the release of the adsorbed cesium ions. This is supported by the significant reduction of the specific area by more than one order of magnitude upon amorphization [7]. Another possible explanation for the reduced desorption of Cs from the thermally treated zeolites is that the exchanged Cs ions may have migrated into the small sodalite cage when the zeolite was heated at a temperature above 900°C. As demonstrated by Norby et al. [34], the Cs ions in the Cs-exchanged zeolite-NaY can migrate from the supercage into the sodalite cage when the material is dehydrated at temperatures above 500°C. Because the diameter of Cs ion (0.34 nm) is large as compared with the 6-ring aperture (0.22 nm) in the sodalite cage, Cs will remain trapped inside the small sodalite cages. The change of desorption behavior of ion-exchanged zeolite upon amorphization is of special interest in a nuclear waste disposal repository where zeolites may be used as waste forms or as a sorption medium for the retardation of radionuclide transport. Since radiation and thermally induced amorphization can easily be achieved in a nuclear waste repository due to the high radiation dose and high temperature, the retention capacity of adsorbed radionuclides may be enhanced. Similar studies have been conducted to investigate the fixation of cesium, strontium and thorium ions in various synthetic zeolites by thermal treatment [7]. The different desorption behaviors in deionized water and $NaNO_3$ solution have suggested that the mechanism of desorption was ion exchange.

4. Conclusions

Both zeolite-NaY and Cs-exchanged zeolite-NaY undergo a crystalline-to-amorphous transformation when exposed to electron irradiation with an energy of 200 keV at a cumulative dose of $\sim 4.0 \times 10^{23}$ e^-/m^2. A fully amorphized zeolite-NaY phase was also obtained by heating the sample up to 900°C in air. At room temperature, the amorphized zeolite-NaY showed a significantly reduced ion exchange capacity as compared with the original crystalline zeolite. The reduction in ion exchange capacity is attributed to the loss of exchangeable cation species and/or the closure of access to exchangeable sites. For Cs-exchanged zeolite-NaY, complete amorphization was achieved when the sample was heated at a higher temperature (1000°C) than the original zeolite-NaY. An XRD study of Cs-exchanged zeolite indicated that a secondary phase formed during the Cs–Na exchange reaction. A desorption study indicates that the thermal treatment of cesium-loaded zeolite-NaY may enhance the retention capacity of loaded Cs ions by trapping these ions inside the resulting amorphous structure.

Acknowledgements

This work was supported by the US DOE/EMSP through grant DE-FG07-97ER45652. We thank Professor Walter J. Weber and Professor Kim Hayes in the Department of Civil and Environmental Engineering, University of Michigan, for the use of their laboratory facilities. The neutron activation analysis was conducted in the Phoenix Memorial Laboratory, and the electron microscopy was conducted in the Electron Micro-Beam Analysis Laboratory of the University of Michigan. We also thank Drs Weilin Huang, Zhi Dang, Chia-chun Chen, Phil Simpson and Leah Minc for their assistance in this work.

References

[1] H.S. Sherry, Molecular Sieve Zeolite, Adv. Chem. Ser. 101, American Chemical Society, Washington, DC (1971) 350.
[2] H. Mimura, K. Akiba, K. Kawamura, J. Radio. Nucl. Chem. 31 (1994) 463.
[3] J.R. Wiley, Ind. Engrg. Chem. Process Des. Dev. 17 (1) (1978) 67.
[4] Anon, Electr. Power Res. Inst. Rep. EPRI NP NO 5991 (1988).
[5] D.C. Grant, A.K. Saha, D.K. Poletz, M.C. Skiba, AIChE Symposium Series 84 (264) (1998) 13.
[6] J.K. Reilly, P.J. Grant, G.J. Quinn, T.C. Runion, K.J. Hofstetter, ASTM Special Technical Publication, ASTM, Philadelphia, PA, USA 2 (1985) 1238.

[7] P.K. Sinha, V. Krishnasamy, J. Nucl. Sci. Tech. 33 (4) (1996) 333.
[8] H. Mimura, T. Kanno, J. Nucl. Sci. Tech. 22 (4) (1985) 284.
[9] H. Mimura, M. Shibata, K. Akiba, J. Nucl. Sci. Tech. 27 (2) (1990) 167.
[10] National Research Council, A Study of the Isolation System for Geologic Disposal of Radioactive Waste, 1983, National Academy Press, Washington, DC.
[11] Civilian Radioactive Waste Management System Management and Operating Contractor, Total System Performance Assessment: An Evaluation of the Potential Yucca Mountain Repository prepared by TRW Environmental Safety systems, 1995.
[12] R.C. Ewing, W.J. Weber, J.F.W. Clinard, Prog. Nucl. Ener. 2 (1995) 63.
[13] R. Csencsits, R. Gronsky, Ultramicroscopy 23 (1987) 421.
[14] M. Pan, Micron 27 (1996) 219.
[15] Y. Sasaki, T. Suzuki, Y. Ikuhara, J. Am. Ceram. Soc. 78 (5) (1995) 1411.
[16] M.M. Treacy, J.M. Newsam, Ultramicroscopy 23 (1987) 411.
[17] Y. Yokota, H. Hashimoto, T. Yamaguchi, Ultramicroscopy 54 (1994) 207.
[18] S.X. Wang, L.M. Wang, R.C. Ewing, Mater. Res. Soc. Symp. 540 (1999) submitted.
[19] S.X. Wang, L.M. Wang, R.C. Ewing, J. Nucl. Mater. 278 (2000) in press.
[20] B.G. Storey, T.R. Allen, Mater. Res. Soc. Symp. 504 (1998).
[21] L.M. Wang, S.X. Wang, R.C. Ewing, Proc. Int. High-Level Radio. Waste Manag. Conf., American Nuclear Society, 1998, p. 772.
[22] D.W. Breck, Zeolite Molecular Sieves – Structure Chemistry and Use, Krieger Publishing, Malabar, FL, 1984.
[23] E. Trif, D. Strugaru, I. Ivan, R. Russu, G. Gheorghe, A. Nicula, J. Thermal Anal. 41 (1994) 871.
[24] V.P. Shiralkar, S.B. Kulkarni, J. Thermal Anal. 25 (1982) 399.
[25] G.V. Tsitsishvili, T.G. Andronikashvili, G.N. Kirov, L.D. Filizova, Nature Zeolite, Ellis Horwood, New York, 1992.
[26] P. Sylvester, A. Clearfield, Solvent Extract. Ion Exchange 16 (6) (1998) 1527.
[27] S.M. DePaoli, J.J. Perona, AIChE J. 42 (12) (1996) 3434.
[28] K.K.S. Pillay, J. Radioanalyt. Nucl. Chem. Articles 102 (1) (1986) 247.
[29] H. Lopez, M.T. Olguin, P. Bosch, S. Bulbulian, J. Radiat. Nucl. Chem. Lett. 200 (1) (1995) 19.
[30] E.A. Daniels, M. Puri, Radiat. Phys. Chem. 27 (3) (1986) 225.
[31] E.A. Daniels, M. Puri, Int. J. Appl. Radiat. Isot. 36 (4) (1985) 291.
[32] E.A. Daniels, M. Puri, Radiat. Eff. 90 (1985) 205.
[33] D. Acosta, G. Vazquez-polo, R. Garcia, V.M. Castano, Radiat. Eff. Def. Solids 127 (1993) 37.
[34] P. Norby, F.I. Poshni, A.F. Gualtieri, J.C. Hanson, C.P. Grey, J. Phys. Chem. B 102 (1998) 839.
[35] P.K. Sinha, P.K. Panicker, R.V. Amalraj, Waste Manag. 15 (2) (1995) 149.
[36] S.H. Sherry, J. Phys. Chem. 70 (4) (1966) 1158.
[37] W.J. Weber, P.M. McGinley, L.E. Katz, Wat. Res. 25 (5) (1991) 499.